Received August 15, 2020, accepted September 6, 2020, date of publication October 6, 2020, date of current version March 9, 2021.

Digital Object Identifier 10.1109/ACCESS.2020.3028869

Performance Analysis of Coherent and Noncoherent Modulation Under I/Q Imbalance Effects

BASSANT SELIM[1], (Member, IEEE), SAMI MUHAIDAT[2,3], (Senior Member, IEEE), PASCHALIS C. SOFOTASIOS[4,5], (Senior Member, IEEE), BAYAN S. SHARIF[4], (Senior Member, IEEE), THANOS STOURAITIS[4], GEORGE K. KARAGIANNIDIS[6], (Fellow, IEEE), AND NAOFAL ALDHAHIR[7], (Fellow, IEEE)

[1]Ericsson AB, Montreal, QC H4S 0B6, Canada
[2]Center for Cyber-Physical Systems, Department of Electrical Engineering and Computer Science, Khalifa University, Abu Dhabi 127788, United Arab Emirates
[3]Department of Systems and Computer Engineering, Carleton University, Ottawa, ON K1S 5B6, Canada
[4]Department of Electrical Engineering and Computer Science, Khalifa University, Abu Dhabi 127788, United Arab Emirates
[5]Department of Electrical Engineering, Tampere University, 33101 Tampere, Finland
[6]Department of Electrical and Computer Engineering, Aristotle University of Thessaloniki, 54124 Thessaloniki, Greece
[7]Department of Electrical Engineering, The University of Texas at Dallas, Richardson, TX 75080, USA

Corresponding author: Bassant Selim (selimpassant@gmail.com)

This work was supported in part by the Khalifa University under Grant KU/RC1-C2PS-T2/8474000137 and Grant KU/FSU-8474000122.

ABSTRACT In this paper, we investigate the effects of in-phase/quadrature-phase imbalance (IQI) on the performance of different modulation schemes under multipath fading channels. In particular, a comprehensive framework for the analysis of coherent and noncoherent modulation with IQI is proposed. Specifically, new moment generating function (MGF) expressions for both point-to-point and multiple antenna systems are derived for the cases of transmitter IQI, receiver IQI, and joint transmitter/receiver IQI. Based on the derived MGFs, new analytical expressions for the corresponding symbol error rate (SER) are derived and are subsequently used to provide deep insights into the effects of IQI on the system performance. It is shown that, while in some cases the SER performance degradation due to IQI is marginal, in other cases, this impairment is more pronounced. Accordingly, IQI compensation is of paramount importance as it can guarantee a reliable communication link. This is particularly important in demanding communication technologies where reduction of latency and complexity are essential.

INDEX TERMS I/Q imbalance, coherent detection, noncoherent detection, RF impairments, symbol error rate.

I. INTRODUCTION

The idea of connecting every single device or ''thing'' to the Internet has led to the development of a revolutionary technology, dubbed as the Internet of things (IoT), that is progressively conquering every aspect of our modern lives. Indeed, given the substantial benefits that can be drawn from this simple, yet mighty, idea, numerous derivatives have emerged, such as the industrial IoT (IIoT), the Internet of vehicles (IoV), the Internet of healthcare things (IoHT), etc. Consequently, future radio networks are envisioned to support heterogeneous devices belonging to different sets of standards and services, which demands for software reconfigurable transceivers that can be adaptive enough to support the associated quality of service requirements. Therefore, given their suitability for high levels of integration as well as their low cost and power consumption, direct conversion transceivers, which do not require any external intermediate frequency/image rejection filters, have attracted considerable attention.

However, from a practical perspective, these transceiver architectures unavoidably experience radio-frequency (RF) front-end related impairments, such as phase noise, DC offset, and in-phase/quadrature-phase imbalances (IQI), which affect the system performance [1]. Here, IQI denotes the mismatch of amplitude and phase between the I/Q branches of direct conversion transceivers, resulting in imperfect image rejection, and hence, degradation in performance [2], [3].

The associate editor coordinating the review of this manuscript and approving it for publication was Zhixiong Peter Li.

Detection schemes can be classified into coherent as well as noncoherent modulation, which depend on the receiver's (RX) ability to extract the carrier phase. In the former, a complete knowledge of the channel state information (CSI) is required at the receiver, which ultimately constitutes a significant issue in emerging communication technologies that are characterized by demanding quality of service requirements, including particularly low latencies. On the contrary, noncoherent detection, which does not require information about the CSI, reduces the receiver complexity by eliminating the need for channel estimation and tracking [4], [5]. Thus. such schemes can be useful in low-power IoT devices [6]. However, this comes at a cost of lower spectral efficiency and/or higher error rate, thus the choice of the best modulation scheme greatly depends on the targeted application. For instance, it was shown that, due to the pilot overhead, noncoherent detection can lead to better spectral efficiency in massive multi-input multi-output (MIMO) systems [7]. The same is the case for low power devices and for ultra low latency telecommunication applications.

A. RELATED WORK

Direct conversion architectures are widely utilized in modern communication transceivers which, due to the problem of mismatch between the I/Q branches, results in residual interference from the image band. Therefore, to address this practical concern, numerous works have been proposed to model, mitigate, or even take advantage of this impairment, see [8] and the references therein.

In [9], the symbol error probability (SEP) of M-ary phase shift keying (PSK) under IQI was investigated for Gaussian channels. Assuming differential quadrature phase shift keying (DQPSK) and Rayleigh fading, the bit error rate (BER) under IQI was derived for single-carrier systems in [10] and multi-carrier systems in [11]. Moreover, in [12], assuming single-carrier modulation, the effects of IQI on the SER of different coherent and noncoherent modulations was investigated. Under the assumption of Weibull fading channels and IQI at the receiver only, the average symbol error rate (SER) of M-ary quadrature amplitude modulation ($M-$QAM) was derived in [13]. Similarly, for M-QAM modulation and Rayleigh fading channels, the error performance of multi-carrier systems and OFDM systems was investigated in [14]–[16] and [17], respectively. For the case of N*Nakagami-m fading, the authors in [18] quantified the effects of IQI on the outage probability of both single-carrier and multi-carrier systems.

Finally, in [19]–[23], the authors analyzed the effects of IQI on the outage performance of non-orthogonal multiple access. IQI has also been studied in half-duplex and full duplex amplify-and-forward and decode-and-forward cooperative systems [24]–[28], two-way relay systems and multi-antenna systems [29]–[37], as well as cognitive radio systems [38]. Finally, the effects of IQI on uplink transmission have been analyzed in the context of massive multi-user MIMO in [39].

B. CONTRIBUTION

To the best of our knowledge, apart from some sporadic results [12], [40], the effects of IQI on noncoherent modulation have been overlooked by the scientific community. Additionally, the existing results on coherent detection consider case-specific scenarios. Thus, they do not provide a holistic treatment of IQI in single and multi-carrier coherent systems. Motivated by this fact, in this article, we extend our work in [12] and investigate the performance of single-carrier and multi-carrier based coherent and noncoherent systems under IQI.

The main objective of this paper is to present a comprehensive framework for the analysis of coherent and noncoherent modulation with different IQI scenarios. To this end, both single-carrier and multi-carrier systems are considered, where, based on the MGF approach, the effects of TX IQI, RX IQI and joint TX/RX IQI on M-PSK, M-DPSK and M-FSK constellations are quantified. The key contributions in this paper are summarized as follows:

- Assuming single-carrier systems over Rayleigh fading channels with TX and/or RX IQI, we derive novel analytic expression for the probability distribution function (PDF) of the signal-to-interference-noise ratio (SINR), based on which the cumulative distribution function (CDF) and MGF expressions are further derived.
- We extend our analysis to the case of multi-carrier transmissions with TX and/or RX IQI and derive novel closed form expressions for the SINR PDF, CDF, and MGF.
- We derive MGF expressions for L-branch MRC receivers and differential Alamouti Space-Time Block Codes (STBC)-OFDM systems under different IQI scenarios.
- Using the derived MGFs, we derive the corresponding SER expressions for M-DPSK, M-PSK and M-FSK constellations.

We quantify the achievable performance of the considered scenarios and develop useful insights of theoretical and practical importance which will be useful in highly demanding emerging technologies. To the best of our knowledge, the contributions of this work are novel and have not been reported in the literature.

C. ORGANIZATION AND NOTATIONS

The rest of this paper is organized as follows: Section II provides a brief overview of the considered modulation schemes. In Sections III and IV, the SINR PDF, CDF, and MGF are derived for single-carrier and multi-carrier systems with IQI, respectively. In addition, Section V presents the SER of M-DPSK, M-PSK, and M-FSK under IQI. The extension to the multiple antenna case is given in Section VI, whereas the corresponding numerical results and discussions are elaborated in Section VII. Finally, closing remarks are given in Section VIII.

Notations: In this article, the subscripts t/r denote the up/down-conversion process at the TX/RX, respectively.

In addition, $(\cdot)^*$ stands for conjugation and $j = \sqrt{-1}$. The operators $\mathbb{E}[\cdot]$ denotes statistical expectation while $|\cdot|$ symbolizes absolute value operations. Finally, $f_X(x)$ and $F_X(x)$ represent the PDF and CDF of X, respectively while $\mathcal{M}_X(s)$ corresponds to the MGF associated with X.

II. SYSTEM MODEL

Considering a single antenna TX/RX where an information symbol s is transmitted over a fading channel h and the noise n is assumed to be additive white Gaussian (AWGN). In the following, we briefly review the signal model of M-ary DPSK, PSK, and FSK modulation schemes.

A. COHERENT DETECTION OF M-PSK SYMBOLS

Assuming M-PSK modulation, it is recalled that

$$\theta_m = \frac{(2m-1)\,\pi}{M}, \qquad m = 1, 2, \ldots, M \tag{1}$$

Hence, the complex baseband signal at the transmitter in the l^{th} symbol interval is given by

$$s_l = A_c \exp(j\theta_l) \tag{2}$$

where $\theta_l \in \theta_m$ is the information phase in the l^{th} symbol. Assuming that the receiver has perfect knowledge of the CSI as well as carrier phase and frequency, the complex baseband signal at the receiver is represented as

$$x_l = A_c \exp(j\theta_l) + n_l. \tag{3}$$

B. NONCOHERENT DETECTION OF M-DPSK SYMBOLS

In DPSK, the information in (1) is encoded using the phase difference between two adjacent transmitted phases. Considering that the channel remains constant over two consecutive symbols, the information sequences at the receiver are decoded without the knowledge of the carrier phase by taking the difference between two adjacent phases [41]. In this context, the information phases $\Delta\theta_l$ are first differentially encoded as:

$$\theta_l = (\theta_{l-1} + \Delta\theta_l) \mod 2\pi \tag{4}$$

where

$$\Delta\theta_m = (2m-1)\pi/M, \quad \text{for } m = 1, \ldots, M, \tag{5}$$

and $\Delta\theta_l$ is the information phase in the l^{th} symbol interval. The modulated symbol s_l is then obtained by applying a phase offset to the previous symbol s_{l-1}, namely,

$$s_l = s_{l-1} \exp(j\theta_l) \tag{6}$$

where $s[1] = 1$. Finally, the decision variable is extracted from the phase difference between two consecutive received symbols as follows

$$\widehat{s_l} = r_{l-1}^* r_l. \tag{7}$$

C. NONCOHERENT DETECTION OF M-FSK SYMBOLS

Assuming M-FSK modulation, the M information frequencies are given by

$$f_m = (2m - 1 - M)\,\Delta f, \qquad m = 1, 2, \ldots, M \tag{8}$$

and thus the l^{th} complex baseband symbol at the transmitter is given by

$$s_l(t) = A_c \exp(j2\pi f_l (t - lT_s)). \tag{9}$$

where $f_l \in f_m$ is the frequency of the l^{th} transmitted symbol and T_s is the symbol period. The decision variable at the receiver is then obtained by multiplying the received signal by the set of complex sinusoids

$$\exp(-j2\pi f_m (t - lT_s)), \qquad m = 1, 2, \ldots, M,$$

and passing them through M matched filters. For orthogonal signals, the frequency spacing is chosen as $\Delta f = N/T_s$, where N is an integer.

III. MGF OF SINGLE-CARRIER SYSTEMS

Single-carrier modulation is receiving increasing attention due to its resilience against RF impairments compared to multi-carrier modulation, see [42] and the references therein. Hence, it is considered more suitable for low complexity and low power applications. Assuming single antenna transceivers, we derive unified closed form expressions for the SINR PDF, CDF, and MGF over flat fading Rayleigh channels and under the influence of IQI at the TX and/or RX.

At the receiver side, the bandpass signal received by the RF front end is passed through processing stages including I/Q demodulation (i.e., down-conversion). Under the assumption of ideal RF front end, the baseband equivalent of the received signal can be written as

$$r_{\text{id}} = hs + n \tag{10}$$

where the index l is dropped for convenience. Moreover, $h \sim \mathcal{CN}(0, 1)$ represents the channel fading gain and $n \sim \mathcal{CN}(0, N_0)$ is the additive white noise term. The instantaneous signal-to-noise ratio (SNR) per symbol is expressed as

$$\gamma_{\text{id}} = \frac{E_s}{N_0} |h|^2 \tag{11}$$

where E_s symbolizes the energy per transmitted symbol. The time-domain baseband representation of the IQI impaired signal is expressed by [43]

$$g_{\text{IQI}} = \mu_{t/r} g_{\text{id}} + \nu_{t/r} g_{\text{id}}^* \tag{12}$$

where g_{id} is the ideal baseband signal and g_{id}^* arises due to IQI. In addition, the corresponding IQI coefficients $\mu_{t/r}$ and $\nu_{t/r}$ are written as

$$\mu_t = \frac{1}{2}(1 + \epsilon_t \exp(j\phi_t)), \tag{13}$$

$$\nu_t = \frac{1}{2}(1 - \epsilon_t \exp(-j\phi_t)), \tag{14}$$

$$\mu_r = \frac{1}{2}(1 + \epsilon_r \exp(-j\phi_r)), \tag{15}$$

and

$$\nu_r = \frac{1}{2}\left(1 - \epsilon_r \exp\left(j\phi_r\right)\right) \tag{16}$$

where $\epsilon_{t/r}$ and $\phi_{t/r}$ correspond to the TX/RX amplitude and phase mismatch levels, respectively. In this work, frequency-independent IQI is assumed; however, the extension to the frequency-dependent case is straightforward, following the approach in [44], [45]. For the ideal case, $\phi_{t/r} = 0°$ and $\epsilon_{t/r} = 1$, which corresponds to $\mu_{t/r} = 1$ and $\nu_{t/r} = 0$. In addition, the TX/RX image rejection ratio (IRR), which quantifies the attenuation of the image band, is given by

$$IRR_{t/r} = \frac{\left|\mu_{t/r}\right|^2}{\left|\nu_{t/r}\right|^2}. \tag{17}$$

A. RECEIVED SINR UNDER IQI

This subsection considers three different cases of practical communication scenarios.

- *Joint TX/RX IQI:* When the TX and RX are impaired by IQI, the SINR can be approximated as [18]

$$\gamma_{\text{IQI}} \approx \frac{|\xi_{11}|^2 + |\xi_{22}|^2}{|\xi_{12}|^2 + |\xi_{21}|^2 + \frac{\Lambda}{\gamma_{\text{id}}}} \tag{18}$$

  where

$$\xi_{11} = \mu_r \mu_t, \tag{19}$$
$$\xi_{22} = \nu_r \nu_t^*, \tag{20}$$
$$\xi_{12} = \mu_r \nu_t, \tag{21}$$

  and

$$\xi_{21} = \nu_r \mu_t^*. \tag{22}$$

- *Ideal TX and RX IQI:* In the case of ideal TX RF front-end and RX IQI. We have $\mu_t = 1$ and $\nu_t = 0$, and therefore the instantaneous SINR per symbol is expressed as [18]

$$\gamma_{\text{IQI}} = \frac{|\mu_r|^2}{|\nu_r|^2 + \frac{\Lambda}{\gamma_{\text{id}}}}. \tag{23}$$

  where $\Lambda = |\mu_r|^2 + |\nu_r|^2$.
- *Ideal RX and TX IQI:* We assume ideal RX RF front-end, while the TX experiences IQI. In this case $\mu_r = 1$ and $\nu_r = 0$, thus the instantaneous SINR at the receiver is given by [18]

$$\gamma_{\text{IQI}} = \frac{|\mu_t|^2}{|\nu_t|^2 + \frac{1}{\gamma_{\text{id}}}}. \tag{24}$$

B. SINR DISTRIBUTION

From (24), (23) and (18), the SINR of single-carrier systems under IQI can be expressed as

$$\gamma_{\text{IQI}} = \frac{\alpha}{\beta + \frac{A}{\gamma_{\text{id}}}} \tag{25}$$

where the parameters α, β, and A are given in Table 1. Hence,

TABLE 1. Single-carrier systems impaired by IQI parameters.

	α	β	A
Joint TX/RX IQI	$\lvert\xi_{11}\rvert^2 + \lvert\xi_{22}\rvert^2$	$\lvert\xi_{12}\rvert^2 + \lvert\xi_{21}\rvert^2$	Λ
RX IQI	$\lvert\mu_r\rvert^2$	$\lvert\nu_r\rvert^2$	Λ
TX IQI	$\lvert\mu_t\rvert^2$	$\lvert\nu_t\rvert^2$	1

the CDF of γ_{IQI} is obtained as

$$F_{\gamma_{IQI}}(x) = F_{\gamma_{id}}\left(\frac{A}{\frac{\alpha}{x} - \beta}\right) \tag{26}$$

where γ_{id} is the IQI free SNR. Since we assume Rayleigh fading, γ_{id} follows an exponential distribution, and therefore, the corresponding SINR CDF is given by

$$F_{\gamma_{IQI}}(x) = 1 - \exp\left(-\frac{A}{\overline{\gamma}\left(\frac{\alpha}{x} - \beta\right)}\right), \quad 0 \le x \le \frac{\alpha}{\beta} \tag{27}$$

where $\overline{\gamma} = E_s/N_0$ is the average SNR. Given that $f_{\gamma_{IQI}}(x) = \frac{d}{dx}F_{\gamma_{IQI}}(x)$, the SINR PDF, under IQI, is given by

$$f_{\gamma_{IQI}}(x) = \frac{\alpha A \exp\left(-\frac{A}{\overline{\gamma}(\frac{\alpha}{x} - \beta)}\right)}{\overline{\gamma}\left(\alpha - x\beta\right)^2} \tag{28}$$

which is valid for $0 \le x \le \frac{\alpha}{\beta}$.

C. MOMENT GENERATING FUNCTION

The MGF is extensively used in the analysis of fading channels [41]. In the following subsection, taking into account the IQI at the TX and/or RX, we derive a generalized closed form expression of the SINR MGF of single-carrier systems. This will be then useful in quantifying the corresponding overall system performance.

Proposition 1: The MGF of the instantaneous SINR of single-carrier systems under IQI is given by

$$\mathcal{M}_{\gamma_{IQI}}(s) = \exp\left(\frac{\alpha}{\beta}s + \frac{A}{\beta\overline{\gamma}}\right)\Gamma\left(1, \frac{A}{\overline{\gamma}\beta}; \frac{s\alpha A}{\beta^2\overline{\gamma}}\right) \tag{29}$$

where $\Gamma(\alpha, x; b)$ denotes the extended upper incomplete Gamma function given by [46]

$$\Gamma(\alpha, x; b) = \int_x^\infty t^{\alpha-1}\exp\left(-t - \frac{b}{t}\right)\mathrm{d}t. \tag{30}$$

Proof: See Appendix A □

IV. MGF OF MULTI-CARRIER SYSTEMS

Multi-carrier systems divide the signal bandwidth among K subcarriers, which provides several advantages including enhanced robustness against multipath fading. Orthogonal frequency division multiplexing (OFDM), a multi-carrier modulation technique, is employed for downlink transmission in Long-Term Evolution (LTE). In this subsection, we derive the SINR PDF, CDF, and MGF of multi-carrier systems over frequency selective channels in the presence of IQI. Let $S = \{-\frac{K}{2}, \cdots, -1, 1, \cdots, \frac{K}{2}\}$ be the set of signals, assuming that all the subcarriers are populated with data and that the channel responses at a given subcarrier and its image

are uncorrelated [18]. In single-carrier systems, IQI causes interference to the signal from its own complex conjugate while in multi-carrier systems, IQI generates interference from the image signal, i.e. the subcarrier k is distorted by the signal at subcarrier $-k$.

A. JOINT TX/RX IMPAIRED BY IQI

Here, we consider the general and most realistic scenario of joint TX/RX IQI. Here, the instantaneous SINR per symbol can be approximated as [18]

$$\gamma \approx \frac{|\xi_{11}|^2 + |\xi_{22}|^2 \frac{\gamma_{\rm id}(-k)}{\gamma_{\rm id}(k)}}{|\xi_{12}|^2 + |\xi_{21}|^2 \frac{\gamma_{\rm id}(-k)}{\gamma_{\rm id}(k)} + \frac{\Lambda}{\gamma_{\rm id}(k)}} \tag{31}$$

where

$$\gamma_{\rm id}(-k) = \frac{E_s}{N_0} |h(-k)|^2 . \tag{32}$$

Therefore, for the case of given $\gamma_{id}(-k)$ and with the aid of (31), the conditional SINR CDF can be expressed as

$$F_{\gamma_{IQI}}(x|y) = 1 - \exp\left(\frac{-x\left(|\xi_{21}|^2 y + \Lambda\right) - |\xi_{22}|^2 y}{\overline{\gamma}\left(|\xi_{11}|^2 - x|\xi_{12}|^2\right)}\right) \tag{33}$$

where $y = \gamma_{id}(-k)$. Consequently, the unconditional CDF is derived by integrating (33) over the Rayleigh PDF, yielding

$$F_{\gamma_{IQI}}(x) = 1 - \frac{\exp\left(-\frac{x\Lambda}{\overline{\gamma}\left(|\xi_{11}|^2 - x|\xi_{12}|^2\right)}\right)}{1 + \frac{x|\xi_{21}|^2 - |\xi_{22}|^2}{\left(|\xi_{11}|^2 - x|\xi_{12}|^2\right)}}, \quad 0 \le x \le \frac{|\xi_{11}|^2}{|\xi_{12}|^2} \tag{34}$$

whereas the SINR PDF is obtained as

$$f_{\gamma_{IQI}}(x) = \frac{\frac{|\xi_{11}|^2\Lambda}{\overline{\gamma}} + \frac{d\left(|\xi_{11}|^2 - x|\xi_{12}|^2\right)}{\frac{|\xi_{11}|^2}{C} + x\left(|\xi_{21}|^2 - |\xi_{12}|^2\right)}}{\left(|\xi_{11}|^2 - x|\xi_{12}|^2\right)\left(\frac{|\xi_{11}|^2}{C} + x\left(|\xi_{21}|^2 - |\xi_{12}|^2\right)\right)} \times \exp\left(\frac{-x\Lambda}{\overline{\gamma}\left(|\xi_{11}|^2 - x|\xi_{12}|^2\right)}\right), \tag{35}$$

which is valid for $0 \le x \le |\xi_{11}|^2/|\xi_{12}|^2$, while C and d are given by

$$C = \frac{|\xi_{11}|^2}{|\xi_{11}|^2 - |\xi_{22}|^2} \tag{36}$$

and

$$d = |\xi_{11}|^2|\xi_{21}|^2 - |\xi_{22}|^2|\xi_{12}|^2. \tag{37}$$

Proposition 2: The MGF of multi-carrier systems impaired by joint TX/RX IQI is given by

$$\mathcal{M}_{\gamma_{IQI}}(s) = C + \frac{|\xi_{12}|^2 C}{s|\xi_{11}|^2} \exp\left(s\frac{|\xi_{11}|^2}{|\xi_{12}|^2} + \frac{\Lambda}{|\xi_{12}|^2\overline{\gamma}}\right) \times \gamma\left(2, s\frac{|\xi_{11}|^2}{|\xi_{12}|^2}; s\frac{|\xi_{11}|^2\Lambda}{|\xi_{12}|^4\overline{\gamma}}\right) \tag{38}$$

for

$$|\xi_{12}|^2 = |\xi_{21}|^2,$$

$$\mathcal{M}_{\gamma_{IQI}}(s) = C + \sum_{p=0}^{\infty} \frac{(-1)^p s^p d^p \exp\left(\frac{\Lambda}{|\xi_{12}|^2\overline{\gamma}} + s\frac{|\xi_{11}|^2}{|\xi_{12}|^2}\right)}{\left(|\xi_{12}|^2 - |\xi_{21}|^2\right)^{p+1} |\xi_{12}|^{2p-2}} \times \gamma\left(1 - p, s\frac{|\xi_{11}|^2}{|\xi_{12}|^2}; s\frac{|\xi_{11}|^2\Lambda}{|\xi_{12}|^4\overline{\gamma}}\right) \tag{39}$$

for

$$\left|\frac{|\xi_{11}|^2|\xi_{21}|^2 - |\xi_{22}|^2|\xi_{12}|^2}{|\xi_{12}|^2 - |\xi_{21}|^2}\right| < |\xi_{11}|^2$$

and

$$\mathcal{M}_{\gamma_{IQI}}(s) = C + \exp\left(s\frac{|\xi_{11}|^2}{|\xi_{12}|^2} + \frac{\Lambda}{|\xi_{12}|^2\overline{\gamma}}\right) \sum_{p=0}^{\infty} \frac{|\xi_{12}|^{2p+4}}{d^{p+1}s^{p+1}} \times \left(|\xi_{21}|^2 - |\xi_{12}|^2\right)^p \gamma\left(p + 2, s\frac{|\xi_{11}|^2}{|\xi_{12}|^2}; s\frac{|\xi_{11}|^2\Lambda}{|\xi_{12}|^4\overline{\gamma}}\right) \tag{40}$$

for

$$\left|\frac{|\xi_{11}|^2|\xi_{21}|^2 - |\xi_{22}|^2|\xi_{12}|^2}{|\xi_{12}|^2 - |\xi_{21}|^2}\right| > |\xi_{11}|^2.$$

In (38)-(40), $\gamma(\alpha, x; b)$ *is the extended lower incomplete Gamma function given by [46]*

$$\gamma(\alpha, x; b) = \int_0^x t^{\alpha-1} \exp\left(-t - \frac{b}{t}\right) {\rm d}t. \tag{41}$$

Proof: The readers are referred to Appendix B. □

B. RX IMPAIRED BY IQI

Assuming that only the RX is impaired by IQI yields the following received instantaneous SINR

$$\gamma_{\rm IQI} = \frac{|\mu_r|^2}{|\nu_r|^2 \frac{\gamma_{\rm id}(-k)}{\gamma_{\rm id}(k)} + \frac{\Lambda}{\gamma_{\rm id}(k)}}. \tag{42}$$

Hence, substituting $\mu_t = 1$ and $\nu_t = 0$ in (34) one obtains

$$F_{\gamma_{IQI}}(x) = 1 - \frac{|\mu_r|^2}{|\mu_r|^2 + x|\nu_r|^2} \exp\left(-\frac{x}{\overline{\gamma}}\left(1 + \frac{|\nu_r|^2}{|\mu_r|^2}\right)\right), \tag{43}$$

which is valid for $0 \le x \le \infty$. By applying algebraic manipulations on (35), the respective SINR PDF is deduced

$$f_{\gamma_{IQI}}(x) = \frac{1 + \frac{|\nu_r|^2}{|\mu_r|^2} + \frac{\overline{\gamma}|\nu_r|^2}{|\mu_r|^2\left(\frac{x|\nu_r|^2}{|\mu_r|^2} + 1\right)}}{\overline{\gamma}\left(\frac{x|\nu_r|^2}{|\mu_r|^2} + 1\right)} \exp\left(-\frac{x\left(\frac{|\nu_r|^2}{|\mu_r|^2} + 1\right)}{\overline{\gamma}}\right) \tag{44}$$

which is valid for $0 \le x \le \infty$.

Finally, from (65) and (44), the corresponding MGF is obtained as

$$\mathcal{M}_{\gamma_{IQI}}(s) = \frac{1+\frac{|\mu_r|^2}{|\nu_r|^2}}{\overline{\gamma}} \int_0^{\infty} \frac{\exp\left(-x\left(\frac{1}{\overline{\gamma}}+\frac{|\nu_r|^2}{\overline{\gamma}|\mu_r|^2}-s\right)\right)}{x+\frac{|\mu_r|^2}{|\nu_r|^2}}dx + \int_0^{\infty} \frac{\exp\left(-x\left(\frac{1}{\overline{\gamma}}+\frac{|\nu_r|^2}{\overline{\gamma}|\mu_r|^2}-s\right)\right)}{\left(x+\frac{|\mu_r|^2}{|\nu_r|^2}\right)^2}dx \quad (45)$$

which with the aid of [47, eq. (3.352.4)] and [47, eq. (3.353.3)], eq. (45) can be expressed by the following closed-form representation

$$\mathcal{M}_{\gamma_{IQI}}(s) = 1 - s\frac{|\mu_r|^2}{|\nu_r|^2}\exp\left(\frac{1}{\overline{\gamma}}+\frac{|\mu_r|^2}{\overline{\gamma}|\nu_r|^2}-\frac{s|\mu_r|^2}{|\nu_r|^2}\right) \times \mathrm{Ei}\left(-\frac{1}{\overline{\gamma}}-\frac{|\mu_r|^2}{\overline{\gamma}|\nu_r|^2}+\frac{s|\mu_r|^2}{|\nu_r|^2}\right) \quad (46)$$

where $\mathrm{Ei}(z)$ denotes the exponential integral function given by [47]

$$\mathrm{Ei}(z) = -\int_{-z}^{\infty} \frac{\exp(-t)}{t}\mathrm{d}t \quad (47)$$

C. TX IMPAIRED BY IQI

Assuming that the TX is subjected to IQI while the RX is ideal, the received instantaneous SINR is obtained as

$$\gamma_{\mathrm{IQI}} = \frac{|\mu_t|^2}{|\nu_t|^2+\frac{1}{\gamma_{\mathrm{id}}(k)}}. \quad (48)$$

Hence, by setting $\mu_r = 1$ and $\nu_r = 0$ in (34), it follows that

$$F_{\gamma_{IQI}}(x) = 1 - \exp\left(-\frac{1}{\overline{\gamma}\left(\frac{|\mu_t|^2}{x}-|\nu_t|^2\right)}\right), \quad 0 \le x \le \frac{|\mu_t|^2}{|\nu_t|^2} \quad (49)$$

which yields straightforwardly the corresponding SINR PDF, namely

$$f_{\gamma_{IQI}}(x) = \frac{|\mu_t|^2 \exp\left(-\frac{1}{\overline{\gamma}\left(\frac{|\mu_t|^2}{x}-|\nu_t|^2\right)}\right)}{\overline{\gamma}\left(|\mu_t|^2-x|\nu_t|^2\right)^2} \quad (50)$$

which is valid for $0 \le x \le |\mu_t|^2/|\nu_t|^2$. It is noted that (50) is similar to (28) for $\alpha = |\mu_t|^2$, $\beta = |\nu_t|^2$, and $A = 1$. Hence, with the aid of (29), the instantaneous SINR MGF of multi-carrier systems experiencing TX IQI only is given by

$$\mathcal{M}_{\gamma_{IQI}}(s) = \exp\left(\frac{|\mu_t|^2}{|\nu_t|^2}s+\frac{1}{|\nu_t|^2\overline{\gamma}}\right)\Gamma\left(1,\frac{1}{\overline{\gamma}|\nu_t|^2};\frac{s|\mu_t|^2}{|\nu_t|^4\overline{\gamma}}\right), \quad (51)$$

which is also novel. The different MGF expressions derived are summarized in Table 2. It is noted that with the aid of the derived MGFs, the SER of various M-ary modulation schemes under different IQI effects as well as multi-channel reception schemes can be readily determined.

V. SYMBOL ERROR RATE ANALYSIS

In this section, we analyze various coherent and noncoherent M-ary modulation schemes and evaluate their SER performance for both single-carrier and multi-carrier-based systems under the effects of IQI.

A. COHERENT M-PSK

The SER of coherently detected M-ary PSK signals in AWGN channels is given by [41, eq. (8.22)]. Assuming fading channels, the average SER is evaluated by averaging [41, eq. (8.22)] over the considered channel's SNR PDF, namely

$$P_{s,PSK} = \frac{1}{\pi}\int_0^{\tilde{M}} \mathcal{M}_{\gamma_{IQI}}\left(-\frac{g}{\sin^2(\theta)}\right)d\theta. \quad (52)$$

where $\tilde{M} = (M-1)\pi/M$ and $g = \sin^2\left(\frac{\pi}{M}\right)$. Therefore, assuming PSK modulation under IQI, the average SER of the different impairment scenarios considered for both single-carrier and multi-carrier systems, can be obtained by substituting the derived MGFs from Table 2 in (52), which, for single-carrier systems, is given by

$$P_{s,PSK} = \frac{1}{\pi}\int_0^{\tilde{M}} \exp\left(-\frac{g\alpha}{\sin^2(\theta)\beta}+\frac{A}{\beta\overline{\gamma}}\right) \times\Gamma\left(1,\frac{A}{\overline{\gamma}\beta};-\frac{g\alpha A}{\sin^2(\theta)\beta^2\overline{\gamma}}\right)d\theta \quad (53)$$

B. COHERENT M-QAM

For M-QAM modulation, the SER of AWGN channels is given by [41, eq. (8.13)]. Under fading conditions and IQI, the average SER is obtained as

$$P_{s,QAM} = \frac{4}{\pi}\underline{M}\int_0^{\frac{\pi}{2}} \mathcal{M}_{\gamma_{IQI}}\left(\frac{3}{2(M-1)\sin^2\theta}\right)d\theta - \frac{4}{\pi}\underline{M}^2\int_0^{\frac{\pi}{4}} \mathcal{M}_{\gamma_{IQI}}\left(\frac{3}{2(M-1)\sin^2\theta}\right)d\theta. \quad (54)$$

where $\underline{M} = \left(\sqrt{M}-1\right)/\sqrt{M}$. The average SER of the different impairment scenarios considered for both single-carrier and multi-carrier systems, can be obtained by substituting the derived MGFs from Table 2 into (54), which, for single-carrier systems, reduces to

$$P_{s,QAM} = \frac{4}{\pi}\underline{M}\int_0^{\frac{\pi}{2}} \exp\left(\frac{3\alpha}{2\beta(M-1)\sin^2\theta}+\frac{A}{\beta\overline{\gamma}}\right) \times\Gamma\left(1,\frac{A}{\overline{\gamma}\beta};\frac{3\alpha A}{\beta^2\overline{\gamma}2(M-1)\sin^2\theta}\right)d\theta - \frac{4}{\pi}\underline{M}^2\int_0^{\frac{\pi}{4}} \exp\left(\frac{3\alpha}{2\beta(M-1)\sin^2\theta}+\frac{A}{\beta\overline{\gamma}}\right) \times\Gamma\left(1,\frac{A}{\overline{\gamma}\beta};\frac{3\alpha A}{\beta^2\overline{\gamma}2(M-1)\sin^2\theta}\right)d\theta. \quad (55)$$

C. DIFFERENTIAL M-PSK

The SER of M-ary PSK with differential detection is given by [41, eq. (8.166)]. Hence, the average SER of M-DPSK under IQI can be evaluated by substituting the derived MGFs from

TABLE 2. SINR MGFs.

	Single-carrier systems	Multi-carrier systems
TX IQI	$\mathcal{M}_{\gamma_{IQI}}(s) = \exp\left(\frac{\lvert\mu_t\rvert^2}{\lvert\nu_t\rvert^2}s + \frac{1}{\lvert\nu_t\rvert^2\overline{\gamma}}\right)\Gamma\left(1, \frac{1}{\overline{\gamma}\lvert\nu_t\rvert^2}; \frac{s\lvert\mu_t\rvert^2}{\lvert\nu_t\rvert^4\overline{\gamma}}\right)$	
RX IQI	$\mathcal{M}_{\gamma_{IQI}}(s) = \exp\left(\frac{\lvert\mu_r\rvert^2 s}{\lvert\nu_r\rvert^2} + \frac{\Lambda}{\lvert\nu_r\rvert^2\overline{\gamma}}\right)\Gamma\left(1, \frac{\Lambda}{\overline{\gamma}\lvert\nu_r\rvert^2}; \frac{s\lvert\mu_r\rvert^2\Lambda}{\lvert\nu_r\rvert^4\overline{\gamma}}\right)$	$\mathcal{M}_{\gamma_{IQI}}(s) = 1 - s\frac{\lvert\mu_r\rvert^2}{\lvert\nu_r\rvert^2}\exp\left(\frac{1}{\overline{\gamma}} + \frac{\lvert\mu_r\rvert^2}{\overline{\gamma}\lvert\nu_r\rvert^2} - \frac{s\lvert\mu_r\rvert^2}{\lvert\nu_r\rvert^2}\right) \times \mathrm{Ei}\left(-\frac{1}{\overline{\gamma}} - \frac{\lvert\mu_r\rvert^2}{\overline{\gamma}\lvert\nu_r\rvert^2} + \frac{s\lvert\mu_r\rvert^2}{\lvert\nu_r\rvert^2}\right)$
Joint IQI	$\mathcal{M}_{\gamma_{IQI}}(s) = \exp\left(\frac{\lvert\xi_{11}\rvert^2+\lvert\xi_{22}\rvert^2}{\lvert\xi_{12}\rvert^2+\lvert\xi_{21}\rvert^2}s + \frac{\Lambda}{(\lvert\xi_{12}\rvert^2+\lvert\xi_{21}\rvert^2)\overline{\gamma}}\right) \times\Gamma\left(1, \frac{\Lambda}{\overline{\gamma}(\lvert\xi_{12}\rvert^2+\lvert\xi_{21}\rvert^2)}; \frac{s(\lvert\xi_{11}\rvert^2+\lvert\xi_{22}\rvert^2)\Lambda}{(\lvert\xi_{12}\rvert^2+\lvert\xi_{21}\rvert^2)^2\overline{\gamma}}\right)$	$\mathcal{M}_{\gamma_{IQI}}(s) = C + \frac{\lvert\xi_{12}\rvert^2}{s(\lvert\xi_{11}\rvert^2-\lvert\xi_{22}\rvert^2)}\exp\left(s\frac{\lvert\xi_{11}\rvert^2}{\lvert\xi_{12}\rvert^2} + \frac{\Lambda}{\lvert\xi_{12}\rvert^2\overline{\gamma}}\right) \times\gamma\left(2, s\frac{\lvert\xi_{11}\rvert^2}{\lvert\xi_{12}\rvert^2}; s\frac{\lvert\xi_{11}\rvert^2\Lambda}{\lvert\xi_{12}\rvert^4\overline{\gamma}}\right),$ for $\lvert\xi_{12}\rvert^2 = \lvert\xi_{21}\rvert^2$
		$\mathcal{M}_{\gamma_{IQI}}(s) = C + \sum_{p=0}^{\infty}\frac{(-s)^p d^p \exp\left(s\frac{\lvert\xi_{11}\rvert^2}{\lvert\xi_{12}\rvert^2}\right)}{(\lvert\xi_{12}\rvert^2-\lvert\xi_{21}\rvert^2)^{p+1}\lvert\xi_{12}\rvert^{2p-2}} \times\exp\left(\frac{\Lambda}{\lvert\xi_{12}\rvert^2\overline{\gamma}}\right)\gamma\left(1-p, s\frac{\lvert\xi_{11}\rvert^2}{\lvert\xi_{12}\rvert^2}; s\frac{\lvert\xi_{11}\rvert^2\Lambda}{\lvert\xi_{12}\rvert^4\overline{\gamma}}\right),$ for $\left\lvert\frac{\lvert\xi_{11}\rvert^2\lvert\xi_{21}\rvert^2-\lvert\xi_{22}\rvert^2\lvert\xi_{12}\rvert^2}{\lvert\xi_{12}\rvert^2-\lvert\xi_{21}\rvert^2}\right\rvert < \lvert\xi_{11}\rvert^2$
		$\mathcal{M}_{\gamma_{IQI}}(s) = C + \sum_{p=0}^{\infty}\frac{\lvert\xi_{12}\rvert^{2p+4}\exp\left(s\frac{\lvert\xi_{11}\rvert^2}{\lvert\xi_{12}\rvert^2}\right)}{(\lvert\xi_{21}\rvert^2-\lvert\xi_{12}\rvert^2)^{-p}d^{p+1}s^{p+1}} \times\exp\left(\frac{\Lambda}{\lvert\xi_{12}\rvert^2\overline{\gamma}}\right)\gamma\left(p+2, s\frac{\lvert\xi_{11}\rvert^2}{\lvert\xi_{12}\rvert^2}; s\frac{\lvert\xi_{11}\rvert^2\Lambda}{\lvert\xi_{12}\rvert^4\overline{\gamma}}\right),$ for $\left\lvert\frac{\lvert\xi_{11}\rvert^2\lvert\xi_{21}\rvert^2-\lvert\xi_{22}\rvert^2\lvert\xi_{12}\rvert^2}{\lvert\xi_{12}\rvert^2-\lvert\xi_{21}\rvert^2}\right\rvert > \lvert\xi_{11}\rvert^2$

Table 2 , which, for multi-carrier systems with TX IQI only, is given by

$$P_{s,DPSK} = \frac{1}{\pi}\int_0^{\tilde{M}} \exp\left(-\frac{\lvert\mu_t\rvert^2 g}{\lvert\nu_t\rvert^2(1+\rho\cos(\theta))} + \frac{1}{\lvert\nu_t\rvert^2\overline{\gamma}}\right) \times\Gamma\left(1, \frac{1}{\overline{\gamma}\lvert\nu_t\rvert^2}, \frac{-g\lvert\mu_t\rvert^2}{(1+\rho\cos(\theta))\lvert\nu_t\rvert^4\overline{\gamma}}, 1\right)d\theta \tag{56}$$

where $\rho = \sqrt{1-g}$.

D. NONCOHERENT M-FSK

The SER of noncoherent detection of orthogonal signals, i.e., M-FSK is given by [41, eq. (8.158)]. Substituting the derived MGF expressions from Table 2 in [41, eq. (8.158)] yields the average SER of single-carrier and multi-carrier systems in the presence of IQI which, for example, for the case of multi-carrier systems with RX IQI only, is given by

$$P_{s,FSK} = \sum_{k=1}^{M-1}\frac{(-1)^{k+1}}{k+1}\binom{M-1}{k} \times\left[1 + \frac{k\lvert\mu_r\rvert^2\mathrm{Ei}\left(-\frac{\Lambda}{\overline{\gamma}\lvert\nu_r\rvert^2} - \frac{k\lvert\mu_r\rvert^2}{(k+1)\lvert\nu_r\rvert^2}\right)}{\exp\left(-\frac{\Lambda}{\overline{\gamma}\lvert\nu_r\rvert^2} - \frac{k\lvert\mu_r\rvert^2}{(k+1)\lvert\nu_r\rvert^2}\right)(k+1)\lvert\nu_r\rvert^2}\right]. \tag{57}$$

VI. EXTENSION TO MIMO SYSTEMS

In this section, we provide deep insights into the performance of multichannel receivers. To this end, we consider the case of an independent but not identically distributed (*i.n.i.d.*) L-branch MRC diversity receiver for coherently detected M-PSK and M-QAM modulations and the case of differential STBC.

A. MAXIMUM RATIO COMBINING

The MRC scheme, which requires the knowledge of the channel fading parameters at the receiver, is the optimal combining scheme at the expense of increased complexity [41], [48]. Here, the receiver coherently combines all received signals, resulting in the following MGF

$$\mathcal{M}_{\gamma_{MRC}}(s) = \mathbb{E}\left[e^{-s\sum_{k=1}^{L}\gamma_k}\right] \tag{58}$$

$$= \prod_{k=1}^{L}\mathcal{M}_{\gamma_k}(s), \tag{59}$$

where γ_k is the instantaneous SNR of the k^{th} branch.

B. DIFFERENTIAL STBC

Here, we consider the differential Alamouti Space-Time Block Codes (STBC)-OFDM system with two transmit antennas and a single receive antenna. Assuming that both the TX and RX are impaired by IQI, the instantaneous SINR at the k^{th} subcarrier is given by [40], [49]

$$\gamma_{IQI}(k) \approx \frac{(1-\epsilon_{TX})^2\left(\gamma_{id_1}(k) + \gamma_{id_2}(k)\right)}{4\left(\frac{1}{\lvert\mu_r\rvert^2\overline{\gamma}} + \frac{\lvert\nu_r\rvert^2}{\lvert\mu_r\rvert^2}\right)} \tag{60}$$

where $\gamma_{id_i}(k)$ is the ideal instantaneous SNR of subcarrier k at the i^{th} antenna and

$$\epsilon_{TX} = 2.5\left(1+\cot\left(\frac{\pi}{M}\right)^2\right)\frac{|\nu_t|^2}{|\mu_t|^2}. \tag{61}$$

From (60), the corresponding SINR MGF is obtained as

$$\mathcal{M}_{\gamma_{\rm IQI}}(s) = \mathcal{M}_{\gamma_{id,1}}\left(s\overline{\Gamma}\right)\mathcal{M}_{\gamma_{id,2}}\left(s\overline{\Gamma}\right) \tag{62}$$

where

$$\overline{\Gamma} = \frac{(1-\epsilon_{TX})^2}{4\left(\frac{1}{|\mu_r|^2\overline{\gamma}}+\frac{|\nu_r|^2}{|\mu_r|^2}\right)} \tag{63}$$

and $\mathcal{M}_{\gamma_{id,j}}$, $j\epsilon\{1,2\}$ is the MGF of the IQI free SNR given by [41]

$$\mathcal{M}_{\gamma_{id,j}}\left(s\overline{\Gamma}\right) = \frac{1}{1-s\overline{\Gamma}} \tag{64}$$

Hence, the corresponding SER is obtained by substituting (62) in the general SER expression for PSK signals in (52). It is noted that the analysis can be easily extended to more than two antenna scenarios [40]. Moreover, the cases of TX IQI only and RX IQI only can be obtained by setting $|\mu_r|^2 = 1, |\nu_r|^2 = 0$ and $|\mu_t|^2 = 1, |\nu_t|^2 = 0$, respectively. To the best of the authors' knowledge, the analytic expressions derived in this section have not been reported in the open technical literature.

VII. SIMULATION AND NUMERICAL RESULTS

In this section, we study the effect of IQI on the performance of single-carrier and multi-carrier systems, assuming M-PSK, M-DPSK, M-QAM, and M-FSK systems over Rayleigh fading channels. To this end, semi-analytical simulations were carried out where random samples of the channel are generated and the corresponding SER is calculated and averaged over a large sample size, i.e. 5×10^7 iterations. For a fair comparison, we normalize the transmitted signal by $|\mu_t|^2+|\nu_t|^2$, $|\mu_r|^2+|\nu_r|^2$, and $\left(|\mu_t|^2+|\nu_t|^2\right)\left(|\mu_r|^2+|\nu_r|^2\right)$ for TX IQI only, RX IQI only, and joint TX/RX IQI, respectively.

Figs. 1−5 and Figs. 6−13 illustrate the SER for single-carrier systems and multi-carrier systems, respectively. Numerical results are shown with lines, while markers represent computer simulation results. For both single-carrier and multi-carrier systems, it is clear that the analytical expressions perfectly match the simulation results for the cases of TX and RX IQI; while for the case of joint TX/RX IQI, the approximation adopted in (18) and (31) and the assumption of uncorrelated subcarriers do not seem to have significant impact on the accuracy of the SER analysis. Furthermore, we notice that, in most cases, the simulation results match the numerical analysis; however, an error that does not exceed 30% is observed in some cases of joint TX/RX IQI, see Figs. 4 and 5.

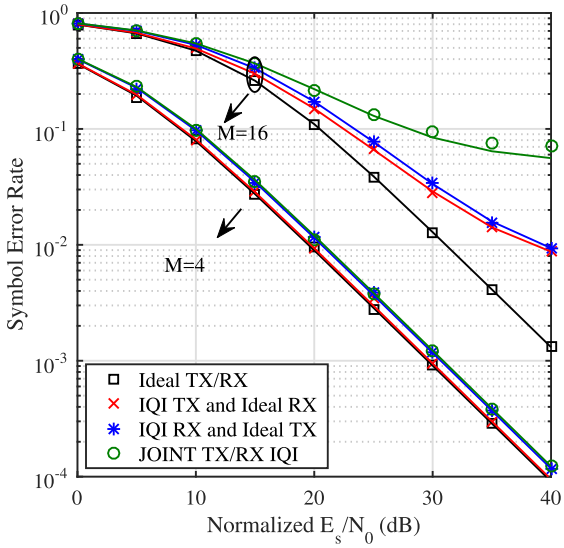

FIGURE 1. Single-carrier system average SER versus normalized E_s/N_0 for M-PSK when $IRR_t = IRR_r = 20dB$ and $\phi = 3°$.

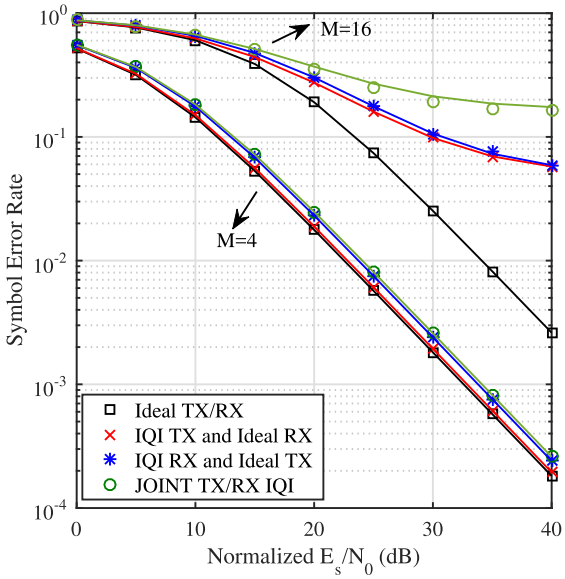

FIGURE 2. Single-carrier system average SER versus normalized E_s/N_0 for M-DPSK when $IRR_t = IRR_r = 20dB$ and $\phi = 3°$.

A. SINGLE-CARRIER SYSTEMS

Assuming single-carrier transmission over flat Rayleigh fading channels, it is first noticed that the impact of RX IQI is more pronounced on the system performance compared to TX IQI. This is due to the fact that RX IQI impairs both the signal and the noise while TX IQI affects the information signal only. However, when the modulation order is increased, as shown in Figs. 1-2, the degradation induced by TX IQI becomes comparable to that observed for the case of RX IQI.

It is also observed that the performance degradation due to IQI greatly depends on the underlying modulation scheme. For instance, in Fig. 4, it is observed that joint TX/RX IQI slightly affects the performance of 32-FSK, while the other three candidate modulation schemes are subject to an error

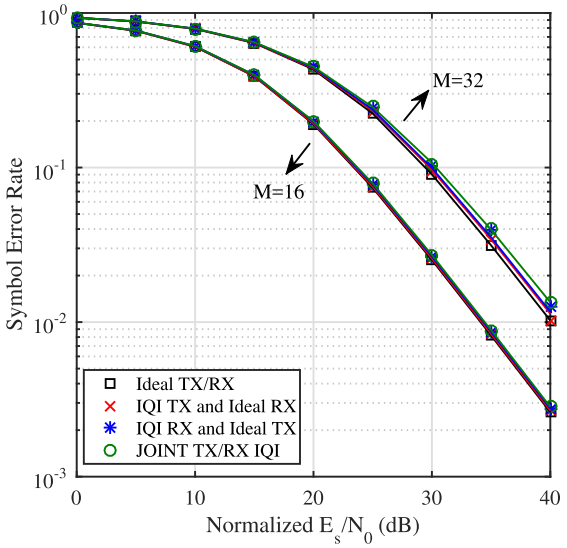

FIGURE 3. Single-carrier system average SER versus normalized E_s/N_0 for M-DPSK when $IRR_t = IRR_r = 35dB$ and $\phi = 1°$.

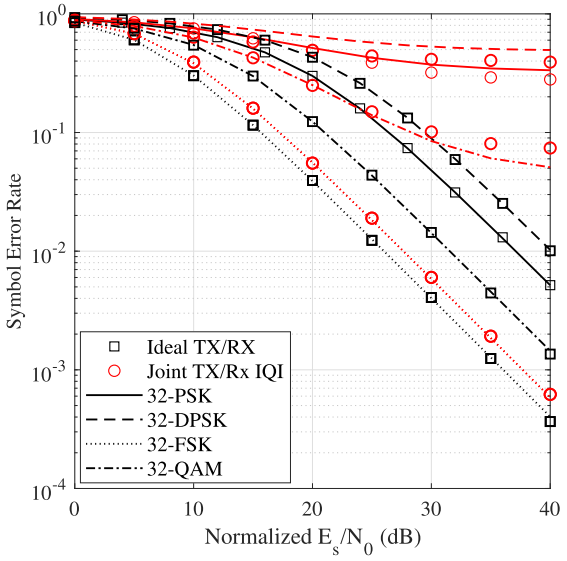

FIGURE 4. Single-carrier system average SER versus normalized E_s/N_0 for 32-PSK, 32-DPSK, 32-FSK and 32-QAM when $IRR_t = IRR_r = 20dB$ and $\phi = 3°$.

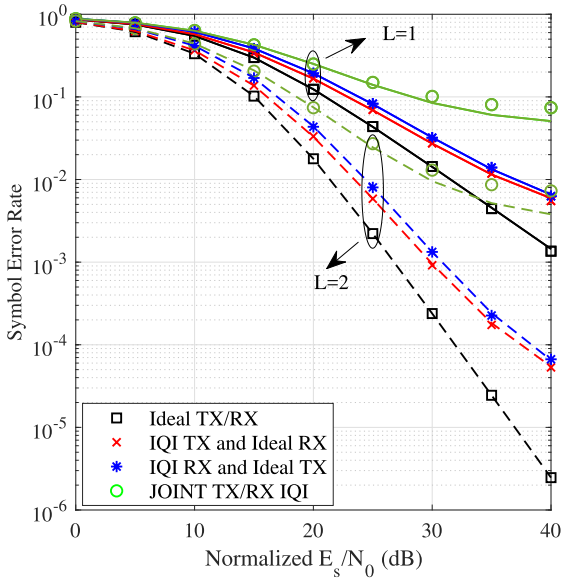

FIGURE 5. Single-carrier system average SER versus normalized E_s/N_0 for L-branch 32-QAM MRC receiver when $IRR_t = IRR_r = 20dB$ and $\phi = 3°$.

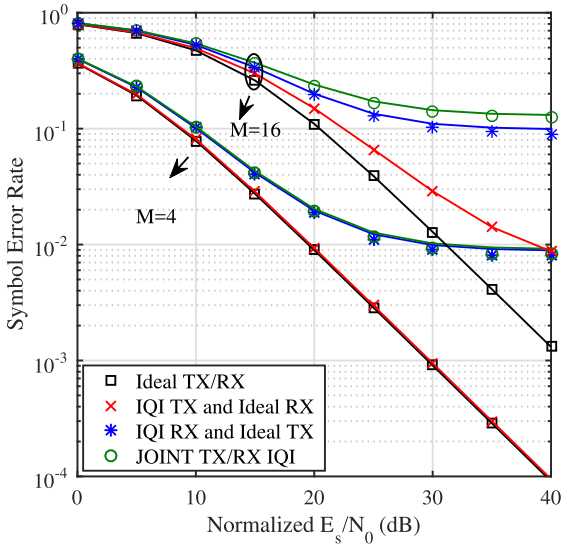

FIGURE 6. Multi-carrier system average SER versus normalized E_s/N_0 for M-PSK when $IRR_t = IRR_r = 20dB$ and $\phi = 3°$.

floor. As shown in Fig. 5, this error floor is manifested in both single-antenna and multi-antenna receivers. This is due to the constant tone spacing in FSK, regardless of the modulation order. Hence, unlike PSK, DPSK, and QAM modulations, it is apparent that the effect of IQI on FSK does not depend on the modulation order. However, for larger M, FSK transmission bandwidth is increased. This is not the case for the other three modulation schemes where the distance between constellation points is highly affected by the modulation order. Consequently, for the considered SNR range, IQI can be considered somehow acceptable i.e., does not cause an error floor, only for $M = 4$ for DPSK and PSK based systems. In fact, for single-carrier systems, for $M = 16$, an error floor is noticed around an SNR of $35dB$ for PSK modulation with joint TX/RX IQI, while for the case of DPSK, the error floor is observed around an SNR of $30dB$ for TX and/or RX IQI. It is also worth noting that for joint TX/RX IQI, the error floor is at a SER of 6×10^{-2} for PSK versus 2×10^{-1} for DPSK. Moreover, it is observed that the level of performance degradation greatly depends on the modulation scheme and/or order and phase and amplitude mismatch level. In particular, it is observed that, in some cases, IQI compensation will only result in added complexity, since the effects of the impairment are negligible. This is evident, particularly when the phase and amplitude mismatch are relatively low, in FSK modulation and low order modulation orders of PSK and DPSK, where the distance between symbols in the constellation is large enough to tolerate the

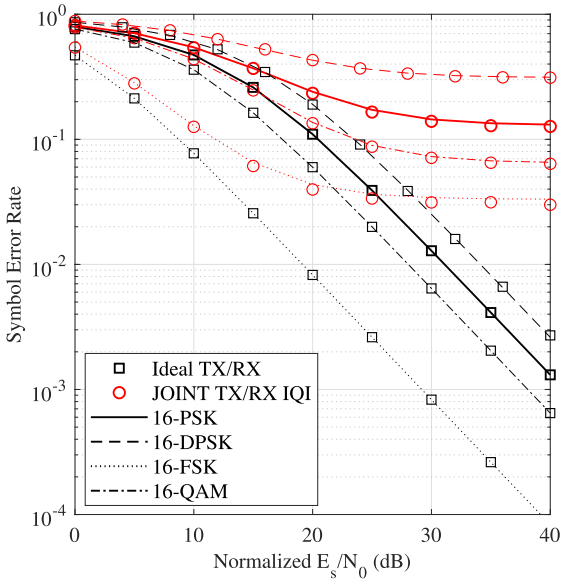

FIGURE 7. Multi-carrier system average SER versus normalized E_s/N_0 for 16-PSK, 16-DPSK, 16-FSK and 16-QAM when $IRR_t = IRR_r = 20dB$ and $\phi = 3°$.

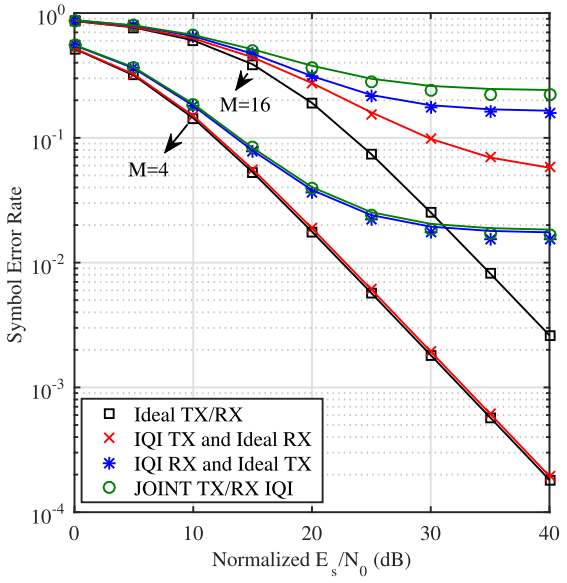

FIGURE 8. Multi-carrier system average SER versus normalized E_s/N_0 for M-DPSK when $IRR_t = IRR_r = 20dB$ and $\phi = 3°$.

error induced by IQI. However, as the mismatch increases, the effects of this impairment become more noticeable and could cause error floor in high modulation orders of phase modulation schemes, which entails compensation in order to achieve a reliable communication link.

B. MULTI-CARRIER SYSTEMS

Here, we assume a multipath channel with 8 independent and identically distributed taps where each tap is a zero-mean complex Gaussian random variable [50]. Without loss of generality, we assume that the number of subcarriers is $K = 32$ and that the SNR reflects the power per subcarrier.

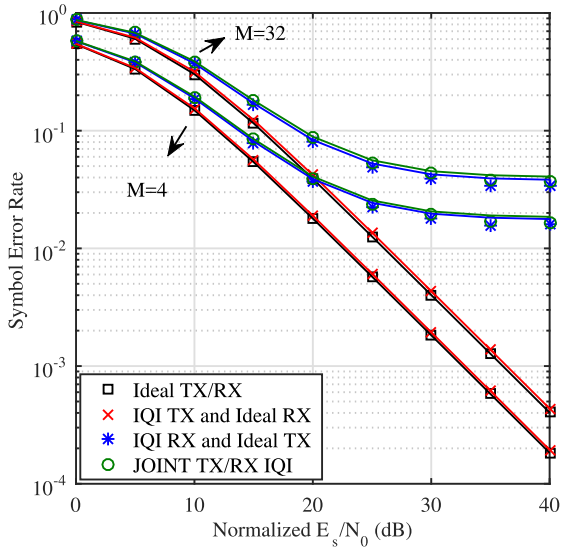

FIGURE 9. Multi-carrier system average SER versus normalized E_s/N_0 for M-FSK when $IRR_t = IRR_r = 20dB$ and $\phi = 3°$.

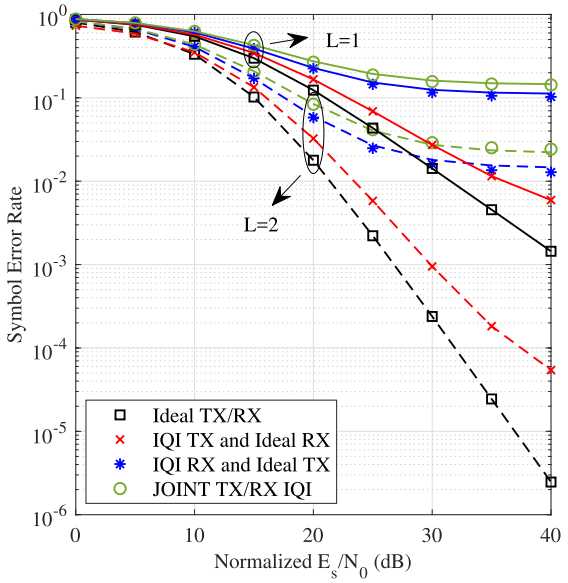

FIGURE 10. Multi-carrier system average SER versus normalized E_s/N_0 for L-branch 32-QAM MRC receiver when $IRR_t = IRR_r = 20dB$ and $\phi = 3°$.

Even though the effects of IQI on the different modulation schemes follow the same trend in multi-carrier systems as in single-carrier systems, it is observed that the impact of IQI on the latter is more pronounced. This is because IQI in multi-carrier systems causes interference from the image subcarrier, which could benefit from better fading conditions than the desired signal. An interesting example is the case of M-FSK constellation, where an error floor is observed in Fig. 9, regardless of the modulation order, for the cases of RX IQI only and joint TX/RX IQI cases. This error floor, which is due to the interference from the image subcarrier in multi-carrier systems, is not observed in single-carrier FSK. In the same context, the error floor for 4-PSK appears at around $25dB$. This error floor is observed for FSK, DPSK,

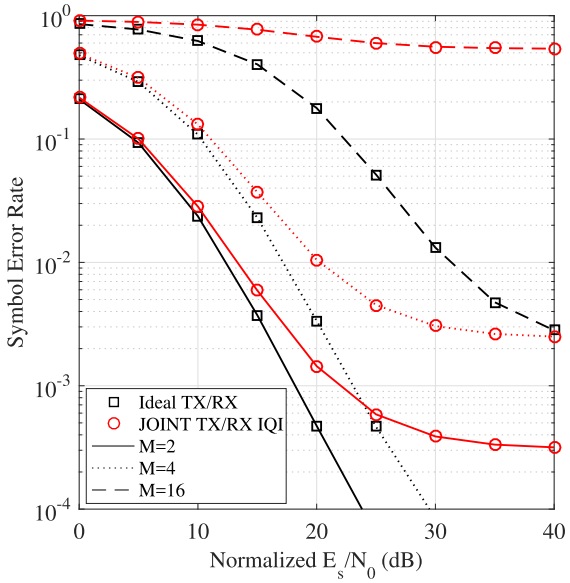

FIGURE 11. Differential Alamouti STBC OFDM SER versus normalized E_s/N_0 for 2-branch receiver when $IRR_t = IRR_r = 20dB$ and $\phi = 3°$.

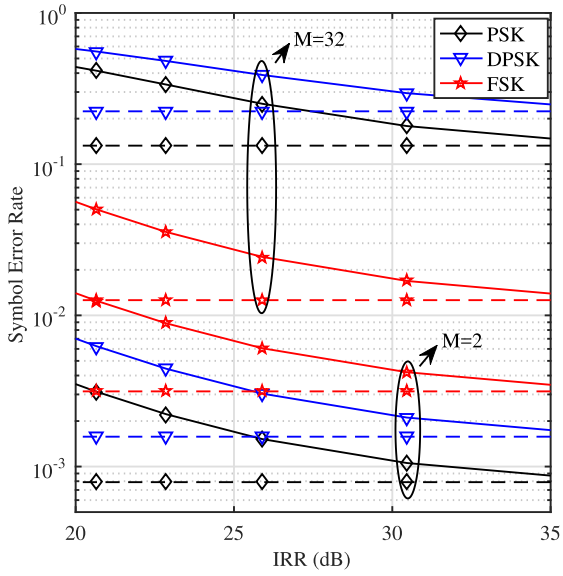

FIGURE 12. Multi-carrier system average SER versus *IRR* for *M*-PSK, *M*-DPSK and *M*-FSK, with RX IQI only, when $E_s/N_0 = 25dB$ and $\phi = 2°$.

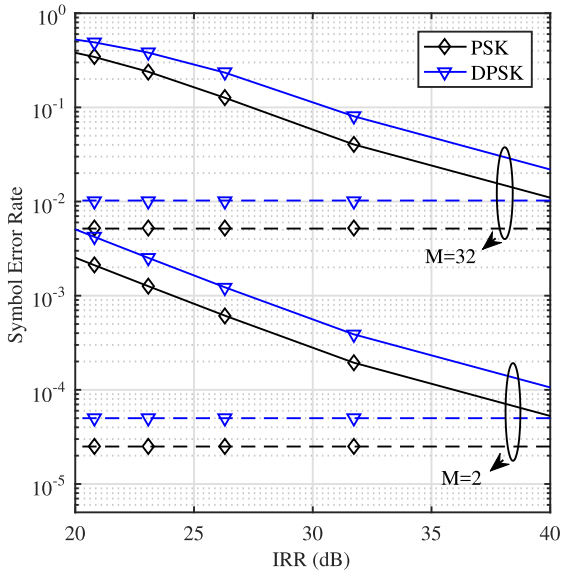

FIGURE 13. Multi-carrier system average SER versus *IRR* for *M*-PSK and *M*-DPSK, with RX IQI only, when $E_s/N_0 = 40dB$ and $\phi = 1°$.

and in 2-branch Differential Alamouti STBC OFDM systems as well. The latter is particularly sensitive to the impairment where it is observed, in Fig. 11, that in case of joint TX/RX IQI, the SER is almost flat for $M = 16$. Moreover, we notice that 4-FSK is the most robust to IQI among the considered modulations, since the error floor appears at around $30dB$.

It is also noted that for $IRR_t = IRR_r = 20dB$, in multi-carrier systems, the effects of IQI at the RX should be compensated in order to achieve a reliable communication link, even in the case of the relatively simple binary modulation schemes and multi-antenna receivers. For these scenarios the amount of performance degradation observed depends on the modulation order, the SNR, the impairment scenario and the IQI level. Hence, in particular cases, such as in low modulation orders of PSK and DPSK modulations, as well as M-FSK, compensation can be implemented at the RX front-end only in order to achieve a reliable performance. On the contrary, in other cases compensation of both TX/RX IQI is required in order to achieve a reliable communication link.

Finally, Fig. 12 and Fig. 13 demonstrate the effects of the *IRR* on the SER of the different considered modulation schemes, when $SNR = 25dB$ and $SNR = 40dB$, respectively. It is assumed that both TX and RX are IQI-impaired and that $IRR_t = IRR_r$. The phase imbalance assumed is 1° in Fig. 12 and 2° in Fig. 13. It is also noted that the continuous lines and dashed lines correspond to the IQI-impaired and ideal cases, respectively. For moderate SNR values, one can see that IQI affects the different modulations schemes in a different manner. For instance, joint TX/ RX IQI exhibits a constant loss in the SER performance of M-FSK regardless of the modulation order, which is not the case when considering phase modulation. Moreover, it is noticed that for lower SNR values, the effects of IQI vanish when the *IRR* is increased; while, for higher SNR values and given that IQI effects dominate noise effects at high SNR, there is a noticeable performance degradation even when considering high *IRR* values.

VIII. CONCLUSION

We presented a framework for the SER analysis of coherent and noncoherent modulation schemes under the effects of IQI. We studied several interesting scenarios, in which TX IQI only, RX IQI only, and joint TX/RX IQI were analyzed and the respective average SER expressions of the underlying schemes were derived for both single-carrier and multi-carrier transmissions. The derived analytical results were corroborated with the corresponding computer simulation results. It was shown that the performance degradation

caused by IQI considerably depends on the system's parameters including the modulation scheme. Moreover, it was demonstrated that increasing the modulation order amplifies the impact of IQI on the system for both coherent and noncoherent systems, while it does not affect the degradation observed in frequency modulation. Additionally, it was shown that the effects of IQI can be quite significant on the SER performance; hence, the optimal compensation strategy greatly depends on the system's parameters. This highlights the importance of accurate IQI characterization in order to achieve a reliable communication link with minimal added complexity.

ACKNOWLEDGMENT

This article was presented in part at the IEEE 87th Vehicular Technology Conference (IEEE VTC Spring), Porto, Portugal, 2018.

APPENDIX A
DERIVATION OF MGF FOR SINGLE-CARRIER SYSTEMS IMPAIRED BY IQI

By recalling that [41]

$$\mathcal{M}_{\gamma_{IQI}}(s) = \int_0^{\infty} \exp(sx) f_{\gamma_{IQI}}(x)\, dx \tag{65}$$

and substituting (28) into (65) yields

$$\mathcal{M}_{\gamma_{IQI}}(s) = \int_0^{\frac{\alpha}{\beta}} \exp(sx) \frac{\alpha A \exp\left(-\frac{A}{\overline{\gamma}\left(\frac{\alpha}{x}-\beta\right)}\right)}{\overline{\gamma}(\alpha - x\beta)^2} dx. \tag{66}$$

Taking $y = \alpha - \gamma\beta$ and after some mathematical manipulations, one obtains

$$\mathcal{M}_{\gamma_{IQI}}(s) = \frac{\alpha A \exp\left(\frac{\alpha\overline{\gamma}s + A}{\beta\overline{\gamma}}\right)}{\overline{\gamma}\beta} \int_0^{\alpha} \exp\left(-\frac{sy}{\beta} - \frac{\alpha A}{\beta\overline{\gamma}y}\right) dy. \tag{67}$$

Finally, by taking $z = \frac{\alpha A}{\beta\overline{\gamma}y}$, (29) is deduced, which completes this proof.

APPENDIX B
DERIVATION OF MGF FOR MULTI-CARRIER SYSTEMS IMPAIRED BY JOINT TX/RX IQI

From (65) and (35), taking $u = \exp(s\gamma)$ and $dv = f_{\gamma}(\gamma)$ and integrating by parts, one obtains

$$\mathcal{M}_{\gamma_{IQI}}(s) = C + s \int_0^{\frac{|\xi_{11}|^2}{|\xi_{12}|^2}} \frac{|\xi_{11}|^2 - x|\xi_{12}|^2}{\frac{|\xi_{11}|^2}{C} + x\left(|\xi_{21}|^2 - |\xi_{12}|^2\right)} \times \exp(sx) \exp\left(-\frac{x}{\overline{\gamma}}\left(\frac{\Lambda}{|\xi_{11}|^2 - x|\xi_{12}|^2}\right)\right) dx \tag{68}$$

For the case of $|\xi_{21}|^2 = |\xi_{12}|^2$ and setting

$$z = |\xi_{11}|^2 - x|\xi_{12}|^2, \tag{69}$$

equation (68) simplifies to

$$\mathcal{M}_{\gamma_{\mathcal{I}\mathcal{Q}\mathcal{I}}}(s) = C + \frac{sC}{|\xi_{12}|^2|\xi_{11}|^2} \exp\left(s\frac{|\xi_{11}|^2}{|\xi_{12}|^2} + \frac{\Lambda}{|\xi_{12}|^2\overline{\gamma}}\right) \times \int_0^{|\xi_{11}|^2} z \exp\left(-z\frac{s}{|\xi_{12}|^2} - \frac{|\xi_{11}|^2\Lambda}{\overline{\gamma}|\xi_{12}|^2 z}\right) dz \tag{70}$$

which considering the change of variable $y = \frac{zs}{|\xi_{12}|^2}$, is equivalent to (38). On the contrary, for $|\xi_{12}|^2 \neq |\xi_{21}|^2$, taking the change of variable in (69), equation (68) becomes

$$\mathcal{M}_{\gamma_{IQI}}(s) = C + \frac{s \exp\left(\frac{\Lambda}{|\xi_{12}|^2\overline{\gamma}} + s\frac{|\xi_{11}|^2}{|\xi_{12}|^2}\right)}{|\xi_{12}|^2 - |\xi_{21}|^2} \times \int_0^{|\xi_{11}|^2} \frac{z \exp\left(-\frac{|\xi_{11}|^2\Lambda}{|\xi_{12}|^2\overline{\gamma}z} - s\frac{z}{|\xi_{12}|^2}\right)}{\frac{d}{|\xi_{12}|^2 - |\xi_{21}|^2} + z} dz \tag{71}$$

where d is given in (37). For the case of

$$\left|\frac{|\xi_{11}|^2|\xi_{21}|^2 - |\xi_{22}|^2|\xi_{12}|^2}{|\xi_{12}|^2 - |\xi_{21}|^2}\right| < |\xi_{11}|^2$$

we expand the involved binomial which yields

$$\mathcal{M}_{\gamma_{IQI}}(s) = C + \sum_{k=0}^{\infty} \frac{(-1)^k s\, d^k \exp\left(\frac{\Lambda}{|\xi_{12}|^2\overline{\gamma}} + s\frac{|\xi_{11}|^2}{|\xi_{12}|^2}\right)}{\left(|\xi_{12}|^2 - |\xi_{21}|^2\right)^{k+1}} \times \int_0^{|\xi_{11}|^2} z^{-k} \exp\left(-\frac{|\xi_{11}|^2\Lambda}{|\xi_{12}|^2\overline{\gamma}z} - s\frac{z}{|\xi_{12}|^2}\right) dz \tag{72}$$

By setting once more $y = xs/|\xi_{12}|^2$, equation (39) is deduced. Meanwhile for

$$\left|\frac{|\xi_{11}|^2|\xi_{21}|^2 - |\xi_{22}|^2|\xi_{12}|^2}{|\xi_{12}|^2 - |\xi_{21}|^2}\right| > |\xi_{11}|^2$$

and expanding the binomial in (71), one obtains the following analytic expression

$$\mathcal{M}_{\gamma_{IQI}}(s) = C + \sum_{k=0}^{\infty} \frac{s \exp\left(\frac{\Lambda + s|\xi_{11}|^2\overline{\gamma}}{|\xi_{12}|^2\overline{\gamma}}\right)\left(|\xi_{21}|^2 - |\xi_{12}|^2\right)^k}{d^{k+1}} \times \int_0^{|\xi_{11}|^2} z^{k+1} \exp\left(-\frac{|\xi_{11}|^2\Lambda}{|\xi_{12}|^2\overline{\gamma}z} - s\frac{z}{|\xi_{12}|^2}\right) dz. \tag{73}$$

Finally, equation (40) is obtained by taking $y = sz/|\xi_{12}|^2$.

REFERENCES

[1] A. Afana, N. Abu-Ali, and S. Ikki, "On the joint impact of hardware and channel imperfections on cognitive spatial modulation MIMO systems: Cramer–Rao bound approach," *IEEE Syst. J.*, vol. 13, no. 2, pp. 1250–1261, Jun. 2019.
[2] S. Mirabbasi and K. Martin, "Classical and modern receiver architectures," *IEEE Commun. Mag.*, vol. 38, no. 11, pp. 132–139, 2000.
[3] S. Bernard, *Digital Communications Fundamentals and Applications*. Upper Saddle River, NJ, USA: Prentice-Hall, 2001.

[4] B. Natarajan, C. R. Nassar, and S. Shattil, "CI/FSK: Bandwidth-efficient multicarrier FSK for high performance, high throughput, and enhanced applicability," *IEEE Trans. Commun.*, vol. 52, no. 3, pp. 362–367, Mar. 2004.

[5] F. F. Digham, M.-S. Alouini, and S. Arora, "Variable-rate variable-power non-coherent M-FSK scheme for power limited systems," *IEEE Trans. Wireless Commun.*, vol. 5, no. 6, pp. 1306–1312, Jun. 2006.

[6] J. Abouei, S. Pasupathy, and K. N. Plataniotis, "Green modulations in energy-constrained wireless sensor networks," *IET Commun.*, vol. 5, no. 2, pp. 240–251, Jan. 2011.

[7] A. Manolakos, M. Chowdhury, and A. J. Goldsmith, "Constellation design in noncoherent massive SIMO systems," in *Proc. IEEE Global Commun. Conf.*, Austin, TX, USA, Dec. 2014, pp. 3690–3695.

[8] B. Selim, P. C. Sofotasios, S. Muhaidat, and G. K. Karagiannidis, "The effects of I/Q imbalance on wireless communications: A survey," in *Proc. IEEE MWSCAS*, Abu Dhabi, United Arab Emirates, Oct. 2016, pp. 1–4.

[9] S. Park and S. H. Cho, "SEP performance of coherent MPSK over fading channels in the presence of Phase/Quadrature error and I-Q gain mismatch," *IEEE Trans. Commun.*, vol. 53, no. 7, pp. 1088–1091, Jul. 2005.

[10] K. Kiasaleh and T. He, "On the performance of DQPSK communication systems impaired by timing error, mixer imbalance, and frequency nonselective slow Rayleigh fading," *IEEE Trans. Veh. Technol.*, vol. 46, no. 3, pp. 642–652, 1997.

[11] B. Selim, P. C. Sofotasios, S. Muhaidat, G. K. Karagiannidis, and B. Sharif, "Performance of differential modulation under rf impairments," in *Proc. IEEE Int. Conf. Commun. (ICC)*, Paris, France, May 2017, pp. 1–6.

[12] B. Selim, S. Muhaidat, P. C. Sofotasios, B. S. Sharif, T. Stouraitis, G. K. Karagiannidis, and N. Al-Dhahir, "Performance analysis of single carrier coherent and noncoherent modulation under I/Q imbalance," in *Proc. IEEE 87th Veh. Technol. Conf. (VTC Spring)*, Jun. 2018, pp. 1–5.

[13] M. Lupupa and J. Qi, "I/Q imbalance in generalized frequency division multiplexing under Weibull fading," in *Proc. IEEE PIMRC*, Hong Kong, Aug. 2015, pp. 471–476.

[14] C.-H. Liu, "Performance analysis of two-sided IQ imbalance effects in OFDM systems," in *Proc. IEEE 20th Int. Symp. Pers., Indoor Mobile Radio Commun.*, Tokyo, Sep. 2009, pp. 938–942.

[15] M. Windisch and G. Fettweis, "Performance degradation due to I/Q imbalance in multi-carrier direct conversion receivers: A theoretical analysis," in *Proc. IEEE Int. Conf. Commun.*, Istanbul, Turkey, Jun. 2006, pp. 257–262.

[16] Y. Zou, M. Valkama, N. Y. Ermolova, and O. Tirkkonen, "Analytical performance of OFDM radio link under RX I/Q imbalance and frequency-selective rayleigh fading channel," in *Proc. IEEE SPAWC*, San Francisco, Jun. 2011, pp. 251–255.

[17] F. J. Lopez-Martinez, E. Martos-Naya, J. F. Paris, and J. T. Entrambasaguas, "Exact closed-form BER analysis of OFDM systems in the presence of IQ imbalances and ICSI," *IEEE Trans. Wireless Commun.*, vol. 10, no. 6, pp. 1914–1922, Jun. 2011.

[18] A.-A.-A. Boulogeorgos, P. C. Sofotasios, B. Selim, S. Muhaidat, G. K. Karagiannidis, and M. Valkama, "Effects of RF impairments in communications over cascaded fading channels," *IEEE Trans. Veh. Technol.*, vol. 65, no. 11, pp. 8878–8894, Nov. 2016.

[19] B. Selim, S. Muhaidat, P. C. Sofotasios, B. S. Sharif, T. Stouraitis, G. K. Karagiannidis, and N. Al-Dhahir, "Performance analysis of non-orthogonal multiple access under I/Q imbalance," *IEEE Access*, vol. 6, pp. 18453–18468, 2018.

[20] B. Selim, S. Muhaidat, P. C. Sofotasios, B. S. Sharif, T. Stouraitis, G. K. Karagiannidis, and N. Al-Dhahir, "Outage probability of single carrier NOMA systems under I/Q imbalance," in *Proc. IEEE Wireless Commun. Netw. Conf. (WCNC)*, Apr. 2018, pp. 1–6.

[21] B. Selim, S. Muhaidat, P. C. Sofotasios, B. S. Sharif, T. Stouraitis, G. K. Karagiannidis, and N. Al-Dhahir, "Outage probability of multi-carrier NOMA systems under joint I/Q imbalance," in *Proc. Int. Conf. Adv. Commun. Technol. Netw. (CommNet)*, Apr. 2018, pp. 1–7.

[22] B. Selim, S. Muhaidat, P. C. Sofotasios, A. Al-Dweik, B. S. Sharif, and T. Stouraitis, "Radio-frequency front-end impairments: Performance degradation in nonorthogonal multiple access communication systems," *IEEE Veh. Technol. Mag.*, vol. 14, no. 1, pp. 89–97, Mar. 2019.

[23] L. Bariah, B. Selim, L. Mohjazi, S. Muhaidat, P. C. Sofotasios, and W. Hamouda, "Pairwise error probability of non-orthogonal multiple access with I/Q imbalance," in *Proc. UK/ China Emerg. Technol. (UCET)*, Aug. 2019, pp. 1–4.

[24] A. Gouissem, R. Hamila, and M. O. Hasna, "Outage performance of cooperative systems under IQ imbalance," *IEEE Trans. Commun.*, vol. 62, no. 5, pp. 1480–1489, May 2014.

[25] M. Mokhtar, N. Al-Dhahir, and R. Hamila, "OFDM full-duplex DF relaying under I/Q imbalance and loopback self-interference," *IEEE Trans. Veh. Technol.*, vol. 65, no. 8, pp. 6737–6741, Aug. 2016.

[26] L. Samara, M. Mokhtar, O. Ozdemir, R. Hamila, and T. Khattab, "Residual self-interference analysis for full-duplex OFDM transceivers under phase noise and I/Q imbalance," *IEEE Commun. Lett.*, vol. 21, no. 2, pp. 314–317, Feb. 2017.

[27] J. Li, M. Matthaiou, and T. Svensson, "I/Q imbalance in AF dual-hop relaying: Performance analysis in Nakagami-*m* fading," *IEEE Trans. Commun.*, vol. 62, no. 3, pp. 836–847, Mar. 2014.

[28] E. Bjornson, M. Matthaiou, and M. Debbah, "A new look at dual-hop relaying: Performance limits with hardware impairments," *IEEE Trans. Commun.*, vol. 61, no. 11, pp. 4512–4525, Nov. 2013.

[29] M. Matthaiou, A. Papadogiannis, E. Bjornson, and M. Debbah, "Two-way relaying under the presence of relay transceiver hardware impairments," *IEEE Commun. Lett.*, vol. 17, no. 6, pp. 1136–1139, Jun. 2013.

[30] J. Li, M. Matthaiou, and T. Svensson, "I/Q imbalance in two-way AF relaying," *IEEE Trans. Commun.*, vol. 62, no. 7, pp. 2271–2285, Jul. 2014.

[31] X. Zhang, M. Matthaiou, M. Coldrey, and E. Björnson, "Impact of residual transmit RF impairments on training-based MIMO systems," *IEEE Trans. Commun.*, vol. 63, no. 8, pp. 2899–2911, Aug. 2015.

[32] N. Kolomvakis, M. Matthaiou, and M. Coldrey, "IQ imbalance in multiuser systems: Channel estimation and compensation," *IEEE Trans. Commun.*, vol. 64, no. 7, pp. 3039–3051, Jul. 2016.

[33] J. Qi and S. Aissa, "Analysis and compensation of I/Q imbalance in MIMO transmit-receive diversity systems," *IEEE Trans. Commun.*, vol. 58, no. 5, pp. 1546–1556, May 2010.

[34] T. C. W. Schenk, E. R. Fledderus, and P. F. M. Smulders, "Performance analysis of zero-IF MIMO OFDM transceivers with IQ imbalance," *J. Commun.*, vol. 2, no. 7, pp. 9–19, 2007.

[35] B. Narasimhan, S. Narayanan, H. Minn, and N. Al-Dhahir, "Reduced-complexity baseband compensation of joint Tx/Rx I/Q imbalance in mobile MIMO-OFDM," *IEEE Trans. Wireless Commun.*, vol. 9, no. 5, pp. 1720–1728, May 2010.

[36] O. Ozdemir, R. Hamila, and N. Al-Dhahir, "I/Q imbalance in multiple beamforming OFDM transceivers: SINR analysis and digital baseband compensation," *IEEE Trans. Commun.*, vol. 61, no. 5, pp. 1914–1925, Feb. 2013.

[37] R. Hamila, O. Ozdemir, and N. Al-Dhahir, "Beamforming OFDM performance under joint phase noise and I/Q imbalance," *IEEE Trans. Veh. Technol.*, vol. 65, no. 5, pp. 2978–2989, May 2016.

[38] A. Mehrabian and A. Zaimbashi, "Spectrum sensing in SIMO cognitive radios under primary user transmitter IQ imbalance," *IEEE Syst. J.*, vol. 13, no. 2, pp. 1210–1218, Jun. 2019.

[39] A. Hakkarainen, J. Werner, K. R. Dandekar, and M. Valkama, "Precoded massive MU-MIMO uplink transmission under transceiver I/Q imbalance," in *Proc. IEEE Globecom Workshops (GC Wkshps)*, Austin, TX, USA, Dec. 2014, pp. 320–326.

[40] L. Chen, A. G. Helmy, G. Yue, S. Li, and N. Al-Dhahir, "Performance analysis and compensation of joint TX/RX I/Q imbalance in differential STBC-OFDM," *IEEE Trans. Veh. Technol.*, vol. 66, no. 7, pp. 6184–6200, Jul. 2017.

[41] M. K. Simon and M.-S. Alouini, *Digital Communication Over Fading Channels*. Hoboken, NJ, USA: Wiley, 2005.

[42] P. Yang, Y. Xiao, Y. L. Guan, K. V. S. Hari, A. Chockalingam, S. Sugiura, H. Haas, M. Di Renzo, C. Masouros, Z. Liu, L. Xiao, S. Li, and L. Hanzo, "Single-carrier SM-MIMO: A promising design for broadband large-scale antenna systems," *IEEE Commun. Surveys Tuts.*, vol. 18, no. 3, pp. 1687–1716, 3rd Quart., 2016.

[43] T. Schenk, *RF Imperfections in High-Rate Wireless Systems: Impact and Digital Compensation*. Dordrecht, The Netherlands: Springer-Verlag, 2008.

[44] L. Anttila, M. Valkama, and M. Renfors, "Frequency-selective I/Q mismatch calibration of wideband direct-conversion transmitters," *IEEE Trans. Circuits Syst. II, Exp. Briefs*, vol. 55, no. 4, pp. 359–363, Apr. 2008.

[45] B. Narasimhan, D. Wang, S. Narayanan, H. Minn, and N. Al-Dhahir, "Digital compensation of frequency-dependent joint Tx/Rx I/Q imbalance in OFDM systems under high mobility," *IEEE J. Sel. Topics Signal Process.*, vol. 3, no. 3, pp. 405–417, Jun. 2009.

[46] M. A. Chaudhry and S. M. Zubair, *On a Class of Incomplete Gamma Functions With Applications*. Boca Raton, FL, USA: CRC Press, 2001.

[47] I. S. Gradshteyn and I. M. Ryzhik, *Table of Integrals, Series, and Products*, 6th ed. New York, NY, USA: Academic, 2000.

[48] B. Selim, O. Alhussein, S. Muhaidat, G. K. Karagiannidis, and J. Liang, "Modeling and analysis of wireless channels via the mixture of Gaussian distribution," *IEEE Trans. Veh. Technol.*, vol. 65, no. 10, pp. 8309–8321, Oct. 2016.
[49] S. M. Alamouti, "A simple transmit diversity technique for wireless communications," *IEEE J. Sel. Areas Commun.*, vol. 16, no. 8, pp. 1451–1458, Oct. 1998.
[50] A. ElSamadouny, A. Gomaa, and N. Al-Dhahir, "A blind likelihood-based approach for OFDM spectrum sensing in the presence of I/Q imbalance," *IEEE Trans. Commun.*, vol. 62, no. 5, pp. 1418–1430, May 2014.

BASSANT SELIM (Member, IEEE) received the master's degree in communication systems from Pierre et Marie Curie (Paris XI) University, Paris, France, in 2011, and the Ph.D. degree from Khalifa University, Abu Dhabi, United Arab Emirates, in 2017. She was a Postdoctoral Fellow with the Ecole de Technologie Suerieure, Montreal, QC, Canada. She is currently a Data Scientist with Ericsson AB, Montreal. Her research interests include wireless communications, radio-frequency impairments, non-orthogonal multiple access, the IoT, and machine learning.

SAMI MUHAIDAT (Senior Member, IEEE) received the Ph.D. degree in electrical and computer engineering from the University of Waterloo, Waterloo, ON, Canada, in 2006.

From 2007 to 2008, he was an NSERC Postdoctoral Fellow with the Department of Electrical and Computer Engineering, University of Toronto, Toronto, ON, Canada. From 2008 to 2012, he was an Assistant Professor with the School of Engineering Science, Simon Fraser University, Burnaby, BC, Canada. He is currently a Professor with Khalifa University, Abu Dhabi, United Arab Emirates, and an Adjunct Professor with Carleton University, Ottawa, ON, Canada. He has authored over 250 technical articles on these topics. His research interests include wireless communications, physical-layer security, the IoT with emphasis on battery-less devices, and machine learning. He is also a member of the Mohammed Bin Rashid Academy of scientists. He was a recipient of several scholarships during his undergraduate and graduate studies and a winner of the 2006 NSERC Postdoctoral Fellowship Competition. He also serves as an Area Editor for the IEEE TRANSACTIONS ON COMMUNICATIONS.

PASCHALIS C. SOFOTASIOS (Senior Member, IEEE) was born in Volos, Greece, in 1978. He received the M.Eng. degree from Newcastle University, U.K., in 2004, the M.Sc. degree from the University of Surrey, U.K., in 2006, and the Ph.D. degree from the University of Leeds, U.K., in 2011.

His M.Sc. studies were funded by a scholarship from UK-EPSRC and his Ph.D. studies were sponsored by UK-EPSRC and Pace plc. He has held academic positions at the University of Leeds, the University of California at Los Angeles, Los Angeles, USA, the Tampere University of Technology, Finland, the Aristotle University of Thessaloniki, Greece, and the Khalifa University of Science and Technology, United Arab Emirates, where he is currently an Assistant Professor. His research interests include broad areas of digital and optical wireless communications, including topics on pure mathematics and statistics. He has been a member and the Co-Chair of the Technical Program Committee of numerous IEEE conferences. He received an Exemplary Reviewer Award from the IEEE COMMUNICATIONS LETTERS in 2012 and the IEEE TRANSACTIONS ON COMMUNICATIONS in 2015 and 2016. He was a co-recipient of the Best Paper Award at ICUFN'13. He also serves as a regular reviewer for several international journals. He also serves as an Editor for the IEEE COMMUNICATIONS LETTERS.

BAYAN S. SHARIF (Senior Member, IEEE) received the B.Sc. degree from Queen's University Belfast, U.K., in 1984, the Ph.D. degree from Ulster University, U.K., in 1988, and the D.Sc. degree from Newcastle University, U.K., in 2013.

From 1990 to 2012, he was the Faculty Member with Newcastle University, where he held a number of appointments, including a Professor of digital communications, the Head of communications and signal processing research, and the Head of the School of Electrical, Electronic and Computer Engineering. He is currently the Dean of the College of Engineering, Khalifa University, Abu Dhabi, United Arab Emirates. His research interests include digital communications with a focus on wireless receiver structures and optimization of wireless networks. He is also a Chartered Engineer and a Fellow of the IET, U.K.

THANOS STOURAITIS received the B.Sc. degree in physics and the M.Sc. degree in electronic automation from the University of Athens, Greece, the M.Sc. degree in electrical and computer engineering from the University of Cincinnati, and the Ph.D. degree from the University of Florida (for which he received the UF Outstanding Ph.D. Dissertation Award).

He joined Khalifa University as a Professor and the Chair of the Department of Electrical Engineering and Computer Science in 2015. He is currently a Professor Emeritus with the University of Patras (UP), where he founded, and directed for 15 years, the International Graduate Program on Signal Processing Systems and Communications, a collaboration of UP and other European and American Universities. He has served as the Director of the Electronics and Computers Division, Department of Electrical and Computer Engineering, UP. He has also served on the National Scientific Board for Mathematics and Informatics of Greece. He was a member of the founding Council of the University of Central Greece. He has also served on the faculties of The Ohio State University, the University of Florida, New York University, and The University of British Columbia. He has authored more than 200 technical articles, as well as, several book chapters and holds one U.S. patent on DSP processor design. He has authored the University of Patras Press book *Digital Signal Processing*, and coauthored the Marcel Dekker Inc. book *Digital Filter Design Software for the IBM PC* and the 2017 *Arithmetic Circuits for DSP Applications* (Wiley-IEEE Press). He has led several DSP processor design projects funded by the European Union, American organizations, and the Greek government and industry, with a total funding totaling more than 3 million EUR. He has delivered more than 10 keynote speeches at international IEEE conferences. His current research interests include signal and image processing systems, application-specific processor technology and design, computer arithmetic, and design and architecture of optimal digital systems with emphasis on cryptographic systems. He is an IEEE Fellow for his contributions in digital signal processing architectures and computer arithmetic. He has also served as the President of the IEEE Circuits and Systems Society for 2012–2013. He received several technical awards, including the IEEE Guillemin-Cauer Best Paper Award. He has also served as the general chair or the technical program chair for several leading conferences. He also serves as Book Series Editor for the River Publishers Series in *Signal, Image and Speech Processing*. He has also served as an Editor and an Associate Editor of several IEEE and IEE journals while he regularly reviews proposals for NSF, the European Commission, and other agencies. He has also served as an external advisor and an examiner for Ph.D. theses in several Universities around the world.

GEORGE K. KARAGIANNIDIS (Fellow, IEEE) was born in Pithagorion, Greece. He received the university diploma and Ph.D. degrees in electrical and computer engineering from the University of Patras, in 1987 and 1999, respectively.

From 2000 to 2004, he was a Senior Researcher with the Institute for Space Applications and Remote Sensing, National Observatory of Athens, Greece. In June 2004, he joined the Faculty Member of the Aristotle University of Thessaloniki, Greece, where he is currently a Professor with the Department of Electrical and Computer Engineering and the Director of the Digital Telecommunications Systems and Networks Laboratory. He is also an Honorary Professor with Southwest Jiaotong University, Chengdu, China. He is the author or coauthor of more than 500 technical articles published in scientific journals and presented at international conferences. He is also the author of the Greek edition of a book on *Telecommunications Systems* and the coauthor of the book *Advanced Optical Wireless Communications Systems* (Cambridge Publications, 2012). His research interests include digital communications systems and signal processing, with emphasis on wireless communications, optical wireless communications, wireless power transfer and applications, communications for biomedical engineering, stochastic processes in biology, and wireless security. He has been involved as the general chair, the technical program chair, and a member of Technical Program Committees in several IEEE and non-IEEE conferences. In the past, he was an Editor in IEEE TRANSACTIONS ON COMMUNICATIONS, a Senior Editor of IEEE COMMUNICATIONS LETTERS, an Editor of the *EURASIP Journal of Wireless Communications & Networks*, and several times Guest Editor in IEEE Selected Areas in Communications. From 2012 to 2015, he was the Editor-in Chief of IEEE COMMUNICATIONS LETTERS. He is one of the highly-cited authors across all areas of Electrical Engineering, recognized from Clarivate Analytics as a Web-of-Science Highly-Cited Researcher in the four consecutive years 2015–2018.

NAOFAL ALDHAHIR (Fellow, IEEE) received the Ph.D. degree in electrical engineering from Stanford University, Stanford, CA, USA.

From 1994 to 2003, he was a Principal Member of the Technical Staff with the GE Research and AT&T Shannon Laboratory. He is currently an Erik Jonsson Distinguished Professor with The University of Texas at Dallas, Richardson, TX, USA. He is the co-inventor of 42 issued U.S. patents and the coauthor of more than 400 articles. He was a co-recipient of four IEEE Best Paper awards. He is also the Editor-in-Chief of IEEE TRANSACTIONS ON COMMUNICATIONS.